Mechanical Characterization of ART-treated Jurkat Cells Using Optical Tweezers

Samaneh Khakshour, Timothy V. Beischlag, Carolyn Sparrey, and Edward J. Park, *Senior Member*, *IEEE*

Abstract— **Acute lymphoid leukemia is a common type of blood cancer and chemotherapy is the initial treatment of choice. Quantifying the effectiveness of a chemotherapeutic drug at the cellular level plays an important role in the process of the treatment. In this study, an optical tweezer was employed to characterize the mechanical properties of Jurkat cells exposed to artesunate (ART) as a chemotherapy. A mathematical model was developed to describe the mechanical characteristics of the cell membrane and its features. By comparing the modeling results against experimental results from the optical tweezer, the elastic modulus of the Jurkat cells before and after ART treatment was calculated. The results demonstrate an increase in the cell stiffness after treatment. Therefore, the elastic modulus of a cell membrane may be a useful biomarker to quantify the effectiveness of a chemotherapeutic agent.**

I. Introduction

Acute lymphoid leukemia (ALL) is a type of blood cancer, which is characterized by the rapid proliferation of transformed lymphoblasts, and is the most common type of blood cancer in children [1]. Early treatment of the disease is essential, since the increased number of malignant cells could spill over into the blood stream and spread to other organs of the body. The most common treatment for leukemia is chemotherapy. Finding and analyzing the effectiveness of drugs with less toxicity on normal cells is indispensable for completely curing the cancer. Artesunate (ART) is an herbal compound which is conventionally used for malaria treatment. It also has anti-cancer effects, especially against leukemic cells (e.g., Jurkat cells–an immortalized line of human T lymphocyte cells) and colon cancer cells, as reported by the Developmental Therapeutics Program of the U.S. National Cancer Institute [2]. Previous studies have revealed the effect of ART on leukemia apoptosis, while having modest side effects on normal cells [3].

One report has suggested that exposing cells to pharmacological agents can cause membrane disorder changing its mechanical properties [4]. In Cai et al. [5], morphological changes of Jurkat cells exposed to ART were analyzed using atomic force microscopy (AFM). Their results demonstrated that ART causes damage to the Jurkat cell membrane and changes the cell's mechanical properties, thus inhibiting cellular proliferation. Based on this report [5], analyzing the mechanical properties of the Jurkat cell membrane may serve as a useful biomarker to quantify the effectiveness of ART on leukemia as a chemotherapeutic agent.

In order to carry out a quantitative study of cell membrane mechanics, a numerical model is needed. In the literature, different mechanical models based on membrane theory have been developed to describe the biomechanical responses of cells. For instance, mechanical properties of microcapsules filled with liquid were analyzed by Carin et al. [6]. A variety of techniques have been used to experimentally characterize the response of suspended cells to mechanical loading. Mechanical characterization has been performed using two indentors or microinjection techniques to investigate suspended tomato cells [7] and zebra fish embryos at different developmental stages [8], respectively. Also, the effect of osmotic condition on red blood cells' (RBCs) mechanical properties was studied by Tan et al. [9] via mechanical modeling and manipulating the RBCs using optical tweezers. The large deformation of a spherical membrane inflated by an incompressible fluid in contact with frictionless rigid conical indenter was analyzed by Sohail and Nadler [10]. As a more recent development, mechanical properties of human embryonic stem cells in cardiac differentiation were analyzed using optical tweezers in Tan et al. [11]. In all of these studies, [6]-[11], the membrane theory is applied to model the mechanical properties of the cells. In membrane theory, the transverse tensions and bending moments are neglected for brevity, and only the in-plane stress resultants are retained in the analysis. However, the biological membrane's bending moment, which arises because of the non-uniform distribution of the stress over the cross section due to the external force, may have an effect on the accuracy and non-singularity of the model [12]. In the current paper, the more comprehensive shell theory is applied to determine the mechanical response of a suspended cell membrane, in order to account for any bending moments that may arise from the use of an optical tweezer in the mechanical characterization of the membrane of Jurkat cells.

To verify the accuracy of the model, an optical tweezer was employed. The optical tweezer is a powerful tool that can be employed to measure the mechanical characteristics of micron-sized objects by applying force and deformation on the order of picoNewtons (pN) and nanometers (nm), respectively. In this paper, mechanical properties of Jurkat cells exposed to different dosages of ART are measured by a

Samaneh Khakshour is with School of Mechatronic Systems Engineering, Simon Fraser University, Surrey, BC V3T 0A3 Canada (corresponding author to provide e-mail: skhaksho@ sfu.ca).

Timothy V. Beischlag is with Faculty of Health Sciences, Simon Fraser University, Burnaby, BC V5A 1S6 Canada (e-mail: tvb@sfu.ca).

Carolyn Sparrey is with School of Mechatronic Systems Engineering, Simon Fraser University, Surrey, BC V3T 0A3 Canada (e-mail: csparrey@sfu.ca).

Edward J. Park is with School of Mechatronic Systems Engineering, Simon Fraser University, Surrey, BC V3T 0A3 Canada (e-mail: ed_park@sfu.ca).

978-1-4244-7929-0/14/$26.00 ©2014 IEEE

combination of optical tweezers and a numerical model. Comparison of the results demonstrates the performance of the proposed model and the effectiveness of the optical tweezer to evaluate the effect of ART on cell membrane mechanical features.

II. Mechanical Model of Cells

Membrane theory has been extensively used for the mechanical characterization of cell membranes [6]-[11]. This theory is a simplified version of the shell theory in which the transverse tensions and bending moments are neglected, and only the in-plane stress resultants are retained in the analysis. In the proposed method, the shell theory is applied to determine a mechanical model of the suspended cell membrane, as a complete analysis, which might include the relative contribution of uneven distribution of stress in our case [12], [13]. Equilibrium equation are used to model the suspended cell deformation behavior as,

$$k_s T_s + k_\varphi T_\varphi = p + \frac{E_B}{\sigma}\left(\frac{d^2(\sigma k_s)}{ds^2} - \frac{d}{ds}\left[\left(k_\varphi\right)\frac{d\sigma}{ds}\right]\right) \quad (1)$$

$$\frac{dT_s}{ds} + \frac{1}{\sigma}\frac{d\sigma}{ds}\left(T_s - T_\varphi\right) = -E_B k_s\left(\frac{dk_s}{ds} + \frac{1}{\sigma}\frac{d\sigma}{ds}\left(k_s - k_\varphi\right)\right) \quad (2)$$

where T_s , T_φ , k_s , k_φ are the principal tensions and curvatures; $\sigma(s)$ is the radial position of the membrane; E_B is the scalar bending modulus; and p is the normal pressure acting on the membrane, and it is calculated as the force of optical tweezer divided by the contact area [12]. The shape for cells before deformation is assumed to be spherical, and Mooney-Rivlin constitutive material is used to represent the cell material [8]. The principal tensions for the Mooney-Rivlin material is expressed as,

$$T_s = 2h_0 C\left(\frac{\lambda_1}{\lambda_2} - \frac{1}{(\lambda_1\lambda_2)^3}\right)\left(1 + \alpha{\lambda_2}^2\right) \quad (3)$$

$$T_\varphi = 2h_0 C\left(\frac{\lambda_2}{\lambda_1} - \frac{1}{(\lambda_1\lambda_2)^3}\right)\left(1 + \alpha{\lambda_1}^2\right) \quad (4)$$

where λ_1 and λ_2 are the principal stretch ratios, C and α are defined in terms of Mooney-Rivlin constants, i.e. C_1 and C_2, where $\alpha = \frac{C_2}{C_1}$ and $C = C_1$, and h_0 is the shell thickness [8]. For homogeneous, incompressible, isotropic elastic material, $C = E/6(1+\alpha)$, where E is the elastic modulus. The set of non-linear differential equations in (1) and (2) are solved using the 4th order Runge-Kutta and multiple shooting methods. C and α are obtained by optimization. The relation between different force and deformation ratios, as well as cell deformation shape can be achieved by solving the above equations.

III. Experiment

A. Optical Tweezer Setup

The optical tweezer experimental setup (mmi Cell Manipulator, MMI AG, Zurich, Switzerland) is illustrated in Fig. 1. A continuous wave 3W, Nd:YAG laser emitting light at a wavelength of 1064 nm was used and the Nikon TE2000 inverted microscope was utilized. A dichroic mirror was used to reflect the laser beam into the 100× objective and focus on the sample. A two dimensional motorized stage driven by stepper motors with 78 nm positioning accuracy was used and the stage movement was controlled by visual feedback. A CCD camera was used for monitoring the experimental process. All the optical and mechanical components were placed on an anti-vibration table.

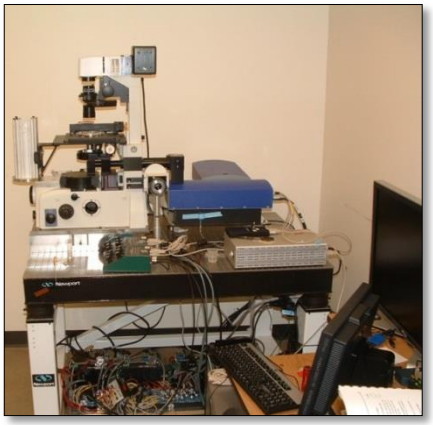

Figure 1. Optical tweezer setup.

B. Experiment Preparation

Jurkat cells were cultured in RPMI-1640 supplemented with 1% penicillin, and 10% FBS at 37°C in a humidified atmosphere of 5% CO2. The exponentially growing cells were cultured in four different dosages of ART (3.125, 6.25, 12.5, 25μg/ml) for 24 h. Microbeads were adhered to cell membranes and were used as a handle for cell manipulation [9]. Streptavidin-coated polystyrene beads (0.5 mg/ml) with radii of 1.55 μm (Bangs Lab, Fishers, IN) were washed three times and incubated with 0.4 mg/ml biotin-conjugated concanavalin A (Con A, Sigma) at 4°C for 40 min with gentle mixing. The antibody-coated beads were then rinsed and added to the washed Jurkat cell suspension, which was incubated at 25°C for 1 h to allow for the adhesion between beads and cells.

C. Force Calibration

The optical tweezers system can be calibrated using an escape force method [14]. In this technique, the force required to move a trapped microbead is calibrated against a known viscous drag force. The calibration procedure involves trapping a microbead in fluid at a measured height, h, above the glass slide surface. The fluid and height of the trapped bead from the slide surface will be kept unchanged throughout calibration and mechanical deformation. As the microscope stage is translated, the fluid exerts a viscous drag force on the trapped bead. The viscous drag force equals the trapping force when the bead just escapes the trap. Using the stage velocity, at the point of escape of the trapped bead, the drag force, which is the opposite of the escape force, is estimated as,

$$F = \frac{6\pi\eta R v}{1 - 9/16(R/h) + 1/8\left(\frac{R}{h}\right)^3 - 45/256\left(\frac{R}{h}\right)^4 - 1/16(R/h)^5} \quad (5)$$

where R is the bead radius, η is fluid viscosity, v is the stage velocity beyond which the bead escaped the trap, and h is the separation distance of the bead from coverslip surface. We used phosphate buffered saline (PBS) as our fluid which has η=0.9 mPa·s at 25°C. During our calibration and cell stretching experiment the separation distance of the bead

from the coverslip was kept at 5 µm. Correlation of laser power with force was determined from repeated trials at five different laser powers (Fig 2).

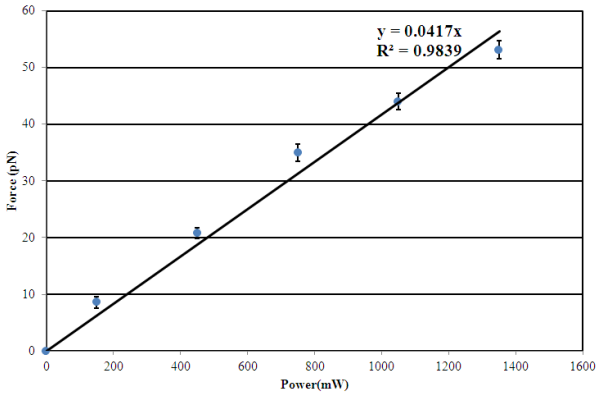

Figure 2.Calibration results of trapping force for a 1.5 µm bead (R^2=0.98).

D. Jurkat Cell Stretching Using the Optical Tweezer

The beads, which were adhered to the Jurkat cell membranes, were used as a handle and trapped by a laser beam to minimize the optical damage. The cell stretching process required anchoring a small portion of the cell to the chamber. In order to attach the cells to the slide, the glass slides were coated with poly-L-lysine (Sigma). The bead which was attached to the cell membrane was trapped by the laser beam. Then, the stage was moved at a velocity of 2 µm/s to diminish the extra viscous drag force exerted on the trapped bead. By moving the stage, the part of the cell that was attached to the chamber will move, while the bead remains fixed in the laser trap, and the Jurkat cells were stretched. The trapping force was equal to the pulling force at the certain maximum deformation. Excess stretch led to escape of the bead from the trap.

Cell deformation was measured at different laser power. Increasing the laser power could lead to more deformation in the cell membrane as illustrated in Fig. 3. The stretching force was acquired by the calibrated force-power relation in Fig. 2. Also, for each level of laser power, the cell deformation was acquired by image processing techniques. During the experiment five different cells were stretched at each laser power, and the results were averaged. Cell deformations were obtained from the stretched cell images when the maximum deformation was observed by image processing.

IV. Results and Discussions

The cell radii were measured for 150 Jurkat cells and the results are presented in Table 1. The contact radius was measured 0.8 µm from the image of an adhered bead to the cell membrane. The membrane thickness was approximated as 7nm [15]. Using these parameters the force-deformation relation based on the proposed mechanical model were obtained. These results are from the assumption of uniform deformation, which is an approximation for now and we will continue to look at the effect of this error in future studies.

To obtain the cell properties from our experimental data, an identification procedure was used. The mechanical properties of cells (C and α) can be identified when the deviation parameter between modeling and experimental data is minimized. The elastic modulus is reported so that we can compare it with previous results in this area.

The mechanical modeling results as well as experimental results for the control group and drug treated Jurkat cells are shown in Fig. 4. Utilizing the experimental results along with modeling, the elastic moduli of un-treated Jurkat cells was estimated to be 0.224±0.04 kPa, which was increased to 0.588±0.11 kPa after treatment with 25 µg/ml ART. These results show similar behavior as 0.254±0.035 kPa and 0.648±0.037 kPa for Jurkat cells and, treated cells which is reported in [5]. A paired-samples t-test was conducted for each group of ART treated cells and control group to compare the effect of ART on the elastic modules of cell membrane. The result for 3.12 ug/ml ART treated cells shows a not-significant difference, $t(4)=2.00$, $p=0.0801$, while showing a significant difference for other groups of treated cells. For example the result for 6.25 µg/ml ART treated cells is $t(4)=5.62$, $p=0.0013$, which suggests that the ART treatment affect the elastic modulus of the Jurkat cells membrane. The elastic moduli of cells exposed to different dosages of ART are illustrated in Fig. 5. These results demonstrate that the ART treated cells' elastic moduli increased in a dose-dependent fashion in contrast to the control group.

Comparing the deformation results for the control and drug treated cells, at the same stretching force, revealed that the control group deformed more severely than the ART-treated cells, therefore the cell stiffness increased with chemotherapy.

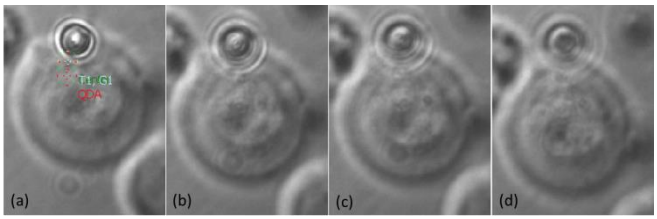

Figure 3. Jurkat cell deformation at four different levels of stretching forces. (a) 0pN, (b)6.3pN, (c) 18.9pN, (d) 31.5pN.

TABLE I. CELL RADII MEASURED FOR 30 JURKAT CELLS IN EACH GROUPS.

Cell	Radius (µm)
Control Group	5.73 ± 0.52
3.12 µg/ml ARTesunated	4.9 ± 0.44
6.25 µg/ml ARTesunated	4.5 ± 0.37
12.5 µg/ml ARTesunated	4.1 ± 0.31
25 µg/ml ARTesunated	3.5 ± 0.26

V. Conclusion

An optical tweezer was used to measure mechanical properties of Jurkat cells exposed to ART. Previous studies [5] showed that ART could inhibit the growth of Jurkat cells, and increasing the concentration of ART could increase the

inhibition rate. The result of this study is in agreement with the previous studies.

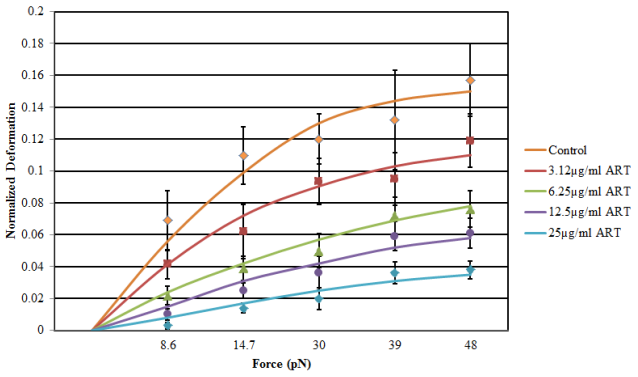

Figure 4. Mechanical responses of Jurkat cells and 3.12 µg/ml, 6.25 µg/ml, 12.5 µg/ml, 25 µg/ml ARTesunated Jurkat cells from both experiment (points) and numerical simulation (solid line). Deformation in the cells is normalized to undeformed cell radius (The error bars are in terms of standard deviation).

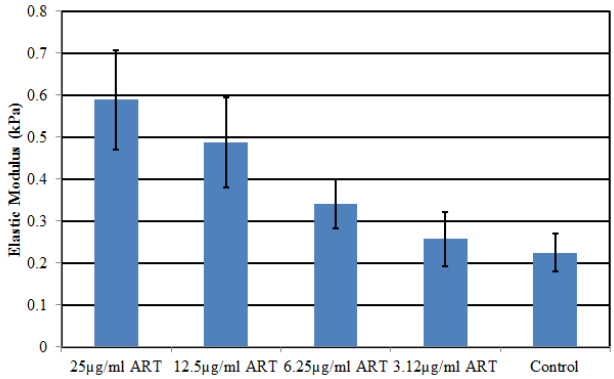

Figure 5. Effect of ART on average elastic modulus of Jurkat cells (The error bars are in terms of standard deviation).

Force-deformation relation was measured for cells exposed to different concentrations of ART. Our results showed that the mechanical properties of the Jurkat cells changed when exposed to ART. Treated cell normalized deformation (0.038 µm) was less than control cell deformation (0.157 µm), when applying 48 pN force. The elastic modulus was 0.588±0.11 kPa in ART treated cells and 0.224±0.04 kPa in the control group. These results clearly show that the cell stiffness increased after the chemotherapy. Therefore, measuring the elastic modulus of cells, with the combined use of the optical tweezer and our numerical model as a tool, could serve as a useful biomarker to quantify the effectiveness of a chemotherapeutic agent.

VI. References

[1] A. Jemal, R. Siegel, E. Ward, T. Murray, J. Xu, and M. Thun, "Cancer statistics," *CA. Cancer J. Clin.,* vol. 57, no. 1, pp. 43-66, 2007.

[2] T. Efferth, H. Dunstan, A. Sauerbrey, H. Miyachi, and C. Chitambar, "The anti-malarial artesunate is also active against cancer," *Int. J. Oncol,* vol. 18, no. 4, pp. 763-773, 2001.

[3] T. Efferth, M. Giaisi, A. Merling, P. Krammer, and A. M. Li-Weber, "Artesunate induces ROS-mediated apoptosis in doxorubicin-resistant T leukemia cells," *PLOS One,* vol. 2, no. 8, pp. 693-693, 2007.

[4] D. Goldstein, "The effects of drugs on membrane fluidity," *Ann. Rev. Pharmacol. Toxicol.,* vol. 24, pp. 43-64, 1984.

[5] X. Cai, S. Gao, J. Cai, Y. Wu, and H. Deng, "Artesunate induced morphological and mechanical changes of jurkat cell studied by AFM," *Scanning,* vol. 31, pp. 83-89, 2009.

[6] M. Carin, D. B-Biesel, F. E-levy, C. Postel, and D.C. Andrei, "Compression of of biocompatible liquid-filled HSA-Alginate capsules: Determination of the membrane mechanical properties," *Biotechnology and Bioengineering,* vol. 82, pp. 207-212, 2003.

[7] C. X. Wang, L. Wang, and C. R. Thomas, "Modeling the mechanical properties of single suspension-cultured tomato cells," *Annals of Botany,* vol. 93, pp. 443-453, 2004.

[8] Y. Tan, D. Sun, W. Huang, and S. H. Cheng, "Mechanical modeling of biological cells in microinjection," *IEEE Transactions on Nanobioscience,* vol. 7, no. 4, pp. 257-267, 2008.

[9] Y. Tan, D. Sun, J. Wang, and W. Huang, "Mechanical characterization of human red blood cells under different osmotic conditions by robotic manipulation with optical tweezers," *IEEE Transactions on Biomedical Engineering,* vol. 57, no, 7, pp. 1816-1826, 2010.

[10] T. Sohail and B. Nadler, "On the contact of an inflated spherical membrane-fluid structure with a rigid conical indenter," *Acta Mech,* pp. 225-235, 2011.

[11] Y. Tan, C. Kong, S. Chen, S. H. Cheng, R. Li, and D. Sun, "Probing the mechanobiological properties of human embryonic stem cells in cardiac differentiation by optical tweezers," *Journal of Biomechanics,* vol. 45, pp. 123-128, 2012.

[12] C. Pozrikidis, *Modelling and simulation of capsules and biological cells*, London: Boca Raton, Fla., 2003.

[13] V. Novozhilov, *Thin Shell Theory*, Groningen: P. Noordhoff, 1964.

[14] K. Svoboda and S. Block, "Biological applications of optical forces," *Annual Review of Biophysics and Biomolecular Structure,* vol. 23, pp. 247-285, 1994.

[15] K. Asami, Y. Takahashi, and S. Takashima, "Dielectric properties of mouse lymphocytes erythrocytes," *Biochim Biophys Acta.,* vol. 1010, no. 1, pp. 49-55, 1989.